# We are IntechOpen,
# the world's leading publisher of
# Open Access books
# Built by scientists, for scientists

## 4,800
Open access books available

## 122,000
International authors and editors

## 135M
Downloads

Our authors are among the

## 154
Countries delivered to

## TOP 1%
most cited scientists

## 12.2%
Contributors from top 500 universities

CLARIVATE ANALYTICS

**BOOK CITATION INDEX**

INDEXED

**WEB OF SCIENCE**™

Selection of our books indexed in the Book Citation Index
in Web of Science™ Core Collection (BKCI)

# Interested in publishing with us?
# Contact book.department@intechopen.com

Numbers displayed above are based on latest data collected.
For more information visit www.intechopen.com

# Application of the Kirkendall Effect to Morphology Control of Nanowires: Morphology Change from Metal Nanowires to Oxide Nanotubes

Ryusuke Nakamura and Hideo Nakajima
*The Institute of Scientific and Industrial Research, Osaka University*
*Japan*

## 1. Introduction

In recent years, considerable effort has been put into the design and fabrication of one-dimensional nanomaterials such as nanorods and nanowires with functional properties. As reviewed in other Chapters, a wide variety of nanowires including inorganic and organic materials have been fabricated and their functional properties have been examined.

Additionally, it is important to obtain nanostructures with a specific size and morphology for expanding the applications of one dimensional nanomaterials. Therefore, the control of the shape of nanowires is one of the most important topics in the current research on nanomaterials. In particular, there is an increasing interest in methods to fabricate hollow nanostructures because their unique shape makes them applicable as delivery vehicles, fillers as well as for catalysis, and is expected to bring about changes in chemical, physical, and catalytic properties. The recent progress in synthesis and applications of hollow nanomaterials including nantoubes has been already reviewed (Fan at al., 2007; Lou et al., 2008; An & Hyeon, 2009).

In general, the most popular concept of methods to fabricate hollow nanostructures can be recognized as the combination of templating, coating and chemical etching. By coating the surface of the template nanowires and removing the template by chemical etching, a wide variety of materials with hollow structures have been successfully synthesized. For example, GaN nanotubes were fabricated through the preparation of ZnO/GaN core/shell structures and the subsequent removal of ZnO nanowires, as shown in Fig. 1 (Goldberger et al., 2003). The arrays of ZnO nanowires were grown on (110) sapphire wafers using a vapour deposition process and then GaN chemical vapor was deposited epitaxially on the ZnO nanowire arrays placed inside a reaction tube. The core part of ZnO can be removed from ZnO/GaN wires by chemical etching with ammonia at high temperature or thermal reduction at high temperatures (for example, 873 K in $H_2$). The synthesis of $Zn_3P_2$, $Cd_3P_2$ (Shen et al., 2006) and $Al_2O_3$ (Ras et al., 2008) nanotubes based on templating and etching method were also reported.
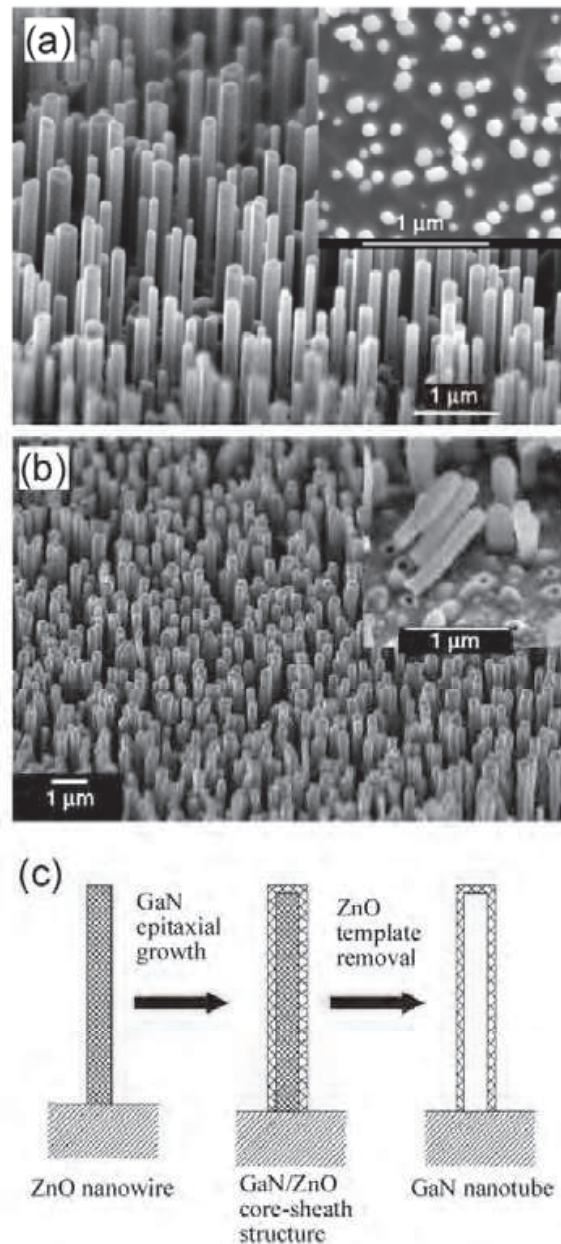
Fig. 1. SEM images of the ZnO nanowire template arrays (a), and the resulting GaN nanotube array (b). Inset in (a) shows cross-sections of the ZnO nanowires. Inset in (b) shows the fractured interface between the GaN nanotubes and the substrate. (c) Schematic illustration of the 'epitaxial casting' process for making single-crystal GaN nanotubes. (Reproduced with permission from the reference (Goldberger et al., 2003))

In addition, different ideas have been applied to the fabrication of hollow nanomaterials. For example, the Kirkendall-effect (Smigelskas & Kirkendall, 1947) related processes have been recognized as one of the useful methods to fabricate oxides, sulfides and phosphides. The Kirkendall effect as a classical phenomenon in metallurgy was established in 1947. It basically refers to a mutual diffusion process through an interface of two metals so that vacancy diffusion occurs to compensate for the unequality of the mass flow and that the initial interface moves. Smigelskas and Kirkendall observed a movement of the initial interface in a Cu/brass diffusion couple, as a result of a faster

diffusion of zinc into the copper than that of copper into the brass (the intrinsic diffusion coefficient of Zn is 2.5 times larger than that of Cu at 785°C.) The Kirkendall experiment demonstrated two important facts: (i) atomic diffusion occurs via vacancies and (ii) each metal diffuses at a different mobility. In some cases, condensation of excess vacancies can give rise to void formation, called 'Kirkendall voids', near original interface and within the faster diffusion side.

Formation of the Kirkendall voids is basically unfavorable from the viewpoint of technological application. The Kirkendall voids should be avoided in the case that interdiffusion occurs at the bonded-interface because they deteriorate the bonding strength of the interface or may cause wire bond failure in integrated circuits. On the other hand, chemists applied the destructive effect constructively for synthesizing hollow nanostructures in a way that the Kirkendall voids coalesce into a single hollow core. In 2004, Yin et al. (2004) demonstrated that initially solid Co nanoparticles transformed into hollow nanoparticles through the reaction with sulfur, oxygen and selenium. The sulfidation of cobalt nanoparticles resulted in the formation of hollow cobalt sulfide of either $Co_3S_4$ or $Co_8S_9$, depending on the molar ration of sulfur and cobalt. During the reaction, the surfaces of cobalt nanoparticles are covered with the sulfide layers and the diffusion of cobalt and sulfur atoms in opposite direction occurs through the sulfide layers. As the reaction proceeds, voids are formed in the cobalt side of the interface because the outward diffusion of cobalt ions is much faster than the inward diffusion of sulfur.

Since Yin et al. (2004) published the results of the synthesis of hollow nanoparticles using the Kirkendall effect, which is a diffusional phenomenon at the interface between different solids, the Kirkendall effect has been applied to the fabrication of a variety of hollow nanoparticles and nanotubes. The first example of the fabrication of nanotubes by the Kirkendall effect is the formation of $ZnAl_2O_4$ spinel nanotubes from $ZnO/Al_2O_3$ core/shell nanowires (Fan et al, 2006). Figure 2 shows TEM images for $ZnAl_2O_4$ nanotubes together with the schematic illustrations of the formation process. As shown in the illustration, the starting material is a ZnO nanowire (10-30 nm thick, up to 20 μm long) coated by $Al_2O_3$(10 nm thick). By annealing the core/shell nanowires in air at 973 K for 3 h, a cylindrical interior nanopore is introduced during the solid state diffusion between ZnO and $Al_2O_3$. $ZnO/Al_2O_3$ reaction is considered as a one-way transfer of ZnO into $Al_2O_3$ in a pseudo binary system.

The Kirkendall effect is related closely to the formation processes of oxide layers on the several metals such as Cu, Ni and Fe; the rapid outward diffusion of metal ions rather than inward oxygen ions through the oxide layers can induce the formation of vacancy clusters, i.e., the Kirkendall voids at the metal sides. Therefore, our focus has been on the fabrication of oxide nanotubes via the oxidation of metal nanowires such as Cu, Ni and Fe, taking vacancy clustering inside metal nanowires due to the Kirkendall effect into consideration.

In this chapter, we will overview our recent results on the morphology changes of metal nanowires via oxidation reactions (Nakamura et al., 2009a, 2009b). The formation mechanisms of oxide nanotubes and porous nanowires will be discussed in terms of diffusion in metals and oxides. Furthermore, the results on the structural stability of nanotubes at high temperatures will be introduced; the morphology change associated with the shrinkage of interior nanopores will be reviewed.
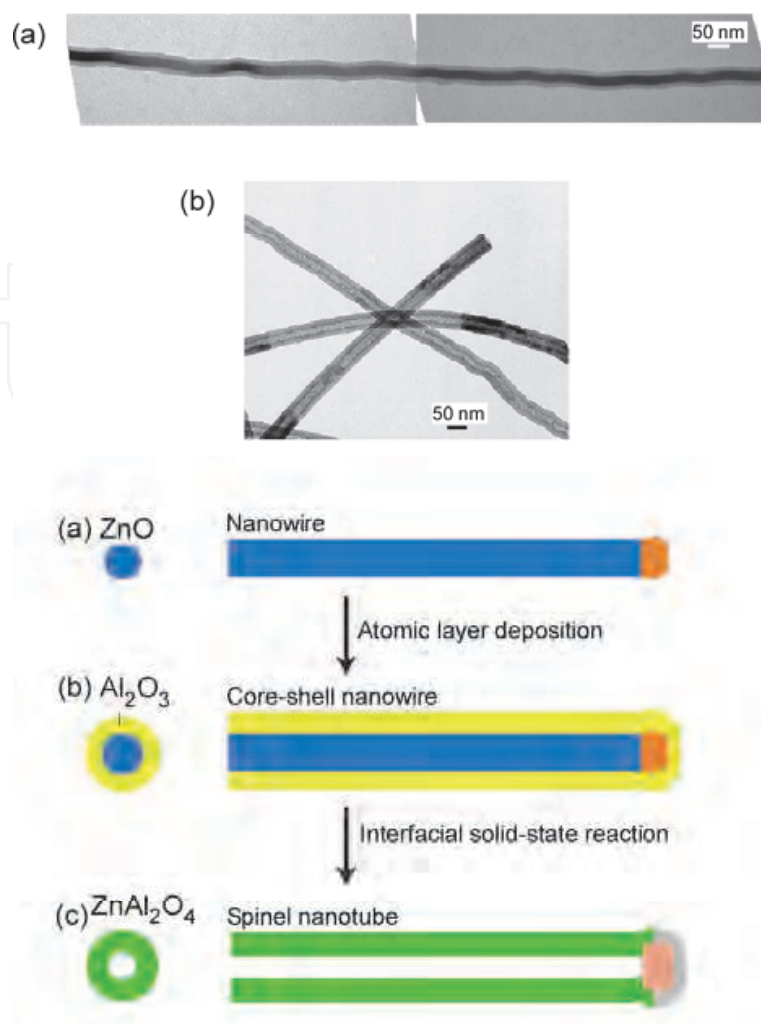
Fig. 2. Transformation of core–shell nanowires to nanotubes by means of the Kirkendall effect (upper). TEM image of an example (a) ZnO-Al$_2$O$_3$ core–shell nanowire and (b) ZnAl$_2$O$_4$ spinel nanotubes. Schematic diagram of the formation process of ZnAl$_2$O$_4$ spinel nanotubes (lower). (a) Single-crystal ZnO nanowires are grown by the vapour–liquid–solid mechanism using Au nanoparticles as a catalyst. (b) The nanowires are coated with a uniform layer of Al$_2$O$_3$ by ALD, forming core–shell ZnO-Al$_2$O$_3$ nanowires. (c) Annealing the core–shell nanowires leads to the formation of ZnAl$_2$O$_4$ nanotubes by a spinel-forming interfacial solid-state reaction involving the Kirkendall effect. (Reproduced with permission from the reference (Fan et al, 2006))

The purpose of this chapter is to show how to fabricate oxide nanotubes through the Kirkendall effect by utilizing metal nanowires as a precursor.

## 2. Shape evolution of metal nanowires due to the Kirkendall effect

### 2.1 Morphology change from metal nanowires during oxidation
In this section, the formation behaviour of interior nanovoids during the oxidation of metal nanowires such as Fe, Cu and Ni will be introduced in 2.1.1 and 2.1.2. The mechanism of interior nanovoids and the difference in void formation behaviour will be discussed in 2.1.3 in terms of diffusion in oxides and metals.

### 2.1.1 Formation of oxide nanotubes via the oxidation of Fe and Cu nanowires

A typical example of the changes in the morphology after the oxidation of iron nanowires from 473 to 573 K is shown in Fig. 3. In our study, metallic nanowires were prepared by electrodeposition through a polycarbonate membrane with a nominal cylindrical pore size of 15 nm and the thickness of 6 μm (Nakamura et al., 2009b). Figure 3 shows bright field images (BFIs) of Fe nanowires (a) before and after oxidation at (b) 473 K for 7.2 ks, (c) 523 K for 3.6 ks, and (d) 573 K for 3.6 ks and their corresponding selected area electron diffraction (SAED) patterns (a')-(d'). Fe nanowires before oxidation had a diameter of 55 nm and a body-centred-cubic structure, as shown in Figs. 3(a) and (a'). Voids were clearly observed along the interface between the Fe nanowire and the outer oxide layer at 473 K for 7.2 ks (Fig. 3(b)) and these were larger at 523 K for 3.6 ks (Fig. 3(c)). Finally, a Fe nanowire turned into a nanotube with a cylindrical nanopore of 40 nm in diameter. The crystal structure of the nanotube was identified to be $Fe_3O_4$ (magnetite) by analyzing the SAED of Fig. 3 (d').
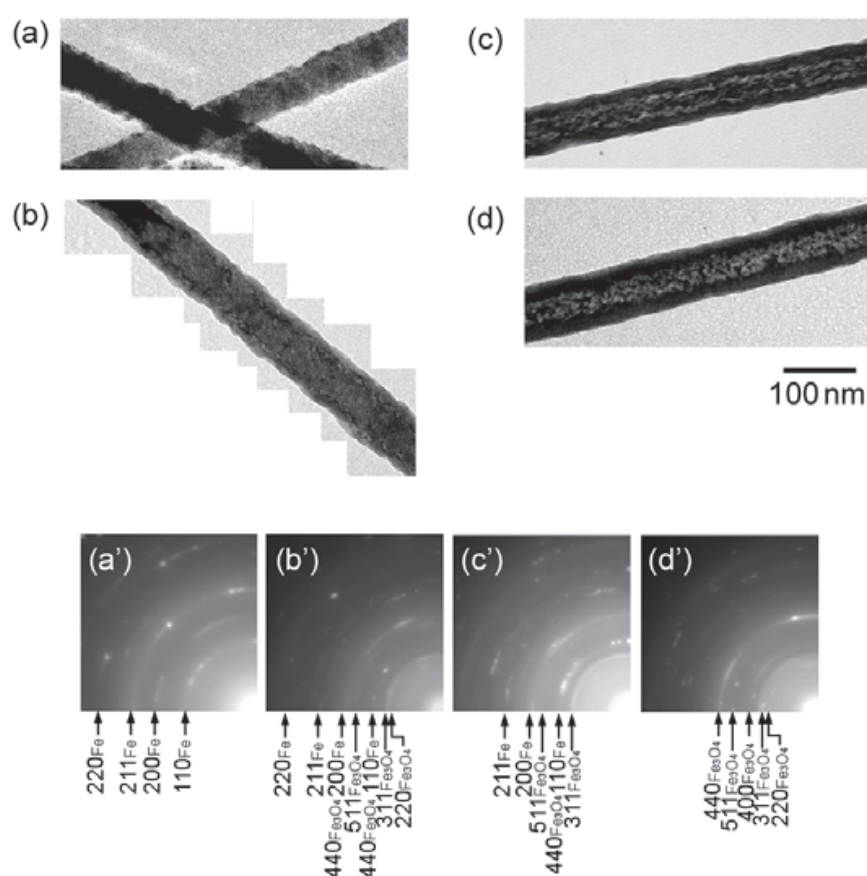


Fig. 3. (a) A bright field image (BFI) of as-deposited Fe nanowires on an amorphous alumina film. (b-d) BFIs of Fe nanowires after oxidation: (b) at 473 K for 7.2 ks, (c) at 523 K for 3.6 ks, and (d) at 573 K for 3.6 ks. (a'-d') are the corresponding selected area electron-diffraction patterns of (a-d). (Reproduced with permission from the reference (Nakamura et al, 2009b))

Figure 4 shows the BFIs of Cu nanowires before (a) and after oxidation at (b,c) 423 and (d) 573 K and their corresponding SAED patterns (a')-(d'). Interior voids with different sizes are fragmentarily generated inside the Cu nanowires after oxidation at 423 K for 1.2 ks, as shown in Fig. 4(b). The oxidized Cu nanowires become nanotubes with a uniform inner and outer diameter at 423 K for 5.4 ks (Fig. 4(c)), as is the case with the oxidation of Fe

nanowires. The crystal structure of the nanotubes obtained via the oxidation of the Cu nanowires at 423 K for 5.4 ks was identified to be $Cu_2O$. $Cu_2O$ transformed into CuO at 573 K while maintaining the nanotube structure, as can be seen in Figs. 4 (d) and (d'). The similarity of the changes in morphology and crystal structure can be also seen for the oxidation of Cu nanoparticles (Nakamura et al., 2008); Cu nanoparticles turn into hollow $Cu_2O$ at around 423 K, followed by the phase transformation from $Cu_2O$ to CuO at 573 K with the hollow structure being maintained.
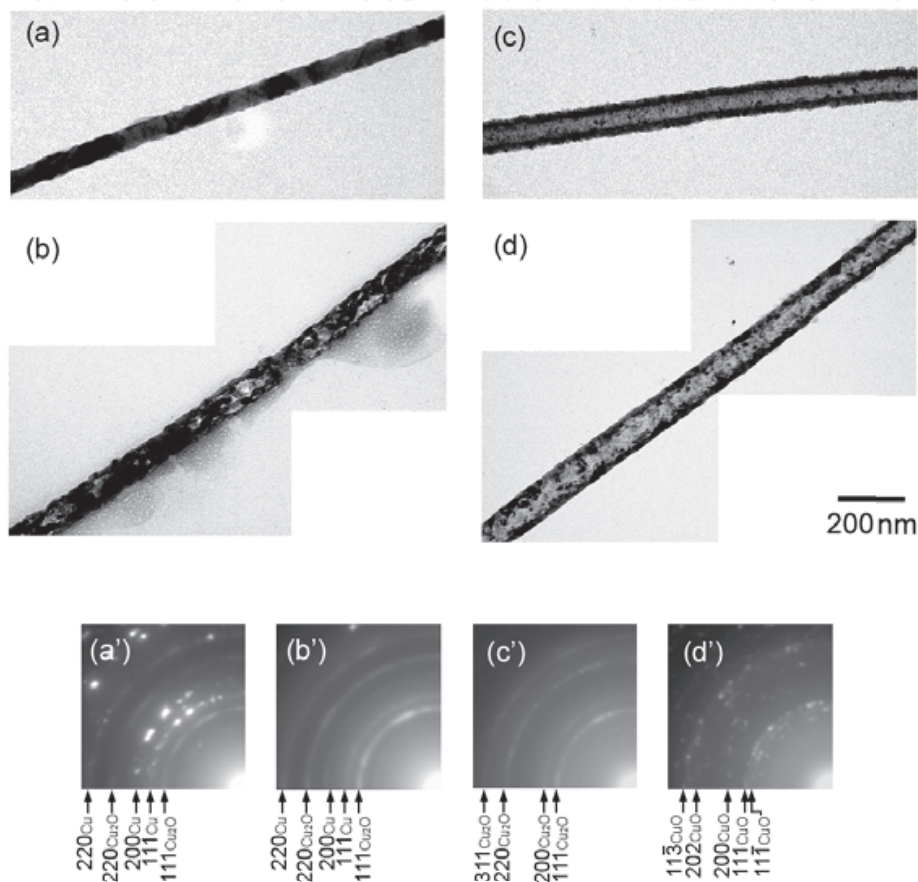


Fig. 4. BFIs of Cu nanowires (a) before oxidation and after oxidation (b) at 423 K for 1.2 ks, (c) at 423 K for 5.4 ks and (d) at 573 K for 3.6 ks and their corresponding SAED patterns (a'-d'). (Reproduced with permission from the reference (Nakamura et al, 2009b))

### 2.1.2 Formation of bamboo-like porous NiO nanowires from Ni nanowires

Figure 5 shows representative electron micrographs of Ni nanowire after oxidation at 673 and 773 K. After oxidation at 673 K for 1.8 ks, large voids are formed at certain places at the interface between an inner remaining Ni wire and the outer oxide layer, as indicated by arrows in Fig. 5(b). The formation behaviour of voids at the interface between Ni and NiO is different from that between Fe and $Fe_3O_4$, where voids are uniformly formed along the interface as apparent from Figs. 3(b) and (c). Ni nanowires became irregularly-shaped bamboo-like NiO with separate interior nanovoids of irregular diameters at 773 K for 3.6 ks, as shown in Fig. 5(c). After the original work carried out by us, Ren at al. (2010) reported similar results on morphology change during the oxidation of Ni nanowires in the temperature range between 623 and 923 K.
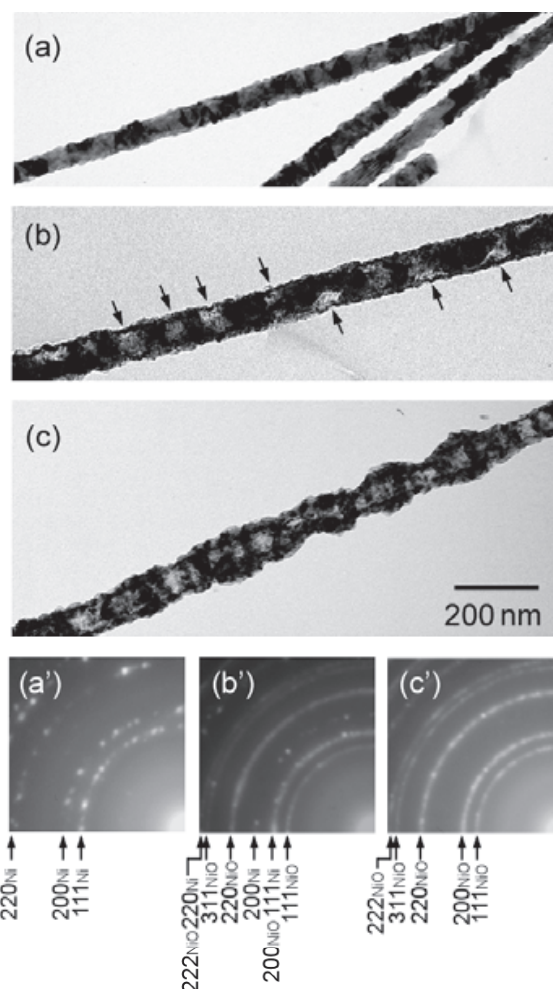
Fig. 5. A typical example of change in morphology of Ni nanowires via oxidation: (a) before oxidation and after oxidation (b) at 673 K for 1.8 ks and (c) at 773 K for 3.6 ks. (Reproduced with permission from the reference (Nakamura et al, 2009b))

### 2.1.3 Formation mechanism of interior nanopores

The formation mechanism of $Fe_3O_4$ and $Cu_2O$ nanotubes is illustrated in Fig. 6 (a); (i) an oxide layer is formed due to the oxidation reaction dominated by the outward diffusion of metal ions through the oxide layer, (ii) voids are generated along the interface due to the inward diffusion of vacancies, which results from the Kirkendall effect, as the oxide layer grows, and (iii) an oxide nanotube with a cylindrical pore is formed after all the metal atoms are consumed by reacting with oxygen.

On the other hand, peculiar behaviour in void formation can be seen in the oxidation of Ni nanowires; the voids grow larger at certain places of the interface between inner Ni and the outer oxide layer during oxidation. Therefore, in the case of Ni, the final morphology is a irregularly-shaped bamboo-like structure with separate interior nanovoids. It can be expected from the TEM image of Fig. 5 (b) that vacancies, which flow into the Ni side as a counter to the outward diffusion of Ni, migrate over a long-range distance, resulting in the growth of voids at certain places. A schematic illustration describing the void formation behaviour during the oxidation of a Ni nanowire is shown in Fig. 6(b). Vacancies, which are formed due to the outward diffusion of Ni at the interface between Ni and NiO, migrate

toward a void (i). The growth of a localized void causes inhomogeneous oxide growth; the growth of the NiO layer is suppressed at the region with a void compared with the region without void in Ni (ii). As a result, a bamboo-like structure with separate interior voids and an irregular shape is formed (iii). In our previous study (Nakamura et al., 2008a), the localization of void formation, which was observed in the oxidation of Ni nanoparticles, was discussed in terms of the mobility of vacancies: vacancies in Ni have sufficient mobility to diffuse over a long-range distance considering the slow growth rate of the NiO layer, resulting in the growth of a single large void at a certain site on the Ni/NiO interface and the formation of an interior nanopore at an off-centred position of hollow NiO. Both the localization of an interior void during the oxidation of Ni nanoparticles and nanowires seem to originate in the high mobility of vacancies in Ni during its oxidation.

(a) Oxidation of Fe and Cu nanowires
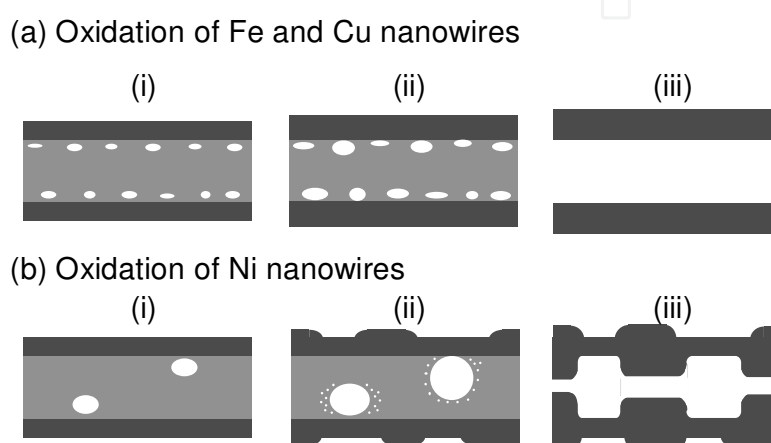


(b) Oxidation of Ni nanowires



Fig. 6. Schematic illustrations of morphology change during oxidation of (a) Fe and Cu and (b) Ni nanowires: (i) the formation of oxide layer due to outward diffusion of metal ions through the initial oxide layer and the formation of voids at the interface between inner metal and outer oxide layer, (ii) the growth of the voids at the interface and (iii) the formation of oxide nanotubes and nanoporous wires with interior nanopore. (Reproduced with permission from the reference (Nakamura et al, 2009b))

## 2.2 Shape evolution via annealing at higher temperatures

According to Gusak et al.(2005), hollow nanostructures are energetically unstable because they include the extra inner surface. They predicted theoretically that hollow nanostructures tend to shrink and collapse as a result of annealing at high temperatures. The authors obtained the experimental results that hollow oxide nanoparticles shrunk and collapsed at higher temperatures (Nakamura et al., 2008b). In order to understand the structural stability of nanotubes of $Fe_3O_4$ and CuO and the bamboo-like structure of NiO, the morphology change after annealing in air at higher temperatures was also investigated (Nakamura et al., 2009b). The results will be reviewed.

## 2.2.1 Shrinkage of interior nanopores

Figure 7 shows the bright field images of (a) CuO nanotubes and (b) the NiO bamboo-like structures after annealing in air at 773 K for 3.6 ks and at 923 K for 3.6 ks, respectively. It is evident that the uniform cylindrical pore in a CuO nanotube, as shown in Fig. 4(d), is almost annihilated, with separate interior voids partly remaining, suggesting that the shrinkage and collapse of CuO nanotubes occur during annealing. In the case of NiO bamboo-like

structures as well as CuO nanotubes, the size of interior separate voids in Fig. 7(b) clearly decreases, compared with those in Fig. 5(d).
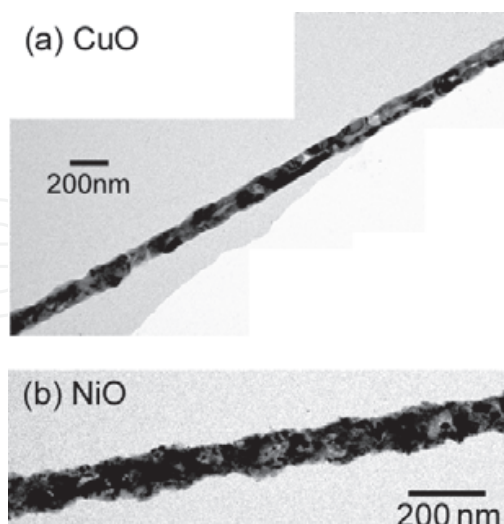


Fig. 7. BFIs of (a) CuO and (b) NiO nanotubes after annealing in air at 773 K for 3.6 ks and at 923 K for 3.6 ks, respectively. (Reproduced with permission from the reference (Nakamura et al, 2009b))

It was demonstrated theoretically (Tu & Gösele, 2005; Gusak et al., 2005; Evteev et al., 2007; Fischer & Svoboda, 2008) and experimentally (Nakamura et al., 2008b) that hollow nanoparticles tend to shrink and collapse at high temperatures because atomic movement occurs to annihilate the inner surface, which originates in the instability of hollow nanoparticles. The shrinkage of interior nanopore(s) was also observed for the oxide nanowires of Fe, Cu and Ni with interior nanopore(s) in our study. It can be concluded, therefore, that both the nanotubes and the hollow nanoparticles tend to shrink and collapse because they are energetically unstable. In our previous study on the structural stability of hollow CuO and NiO nanoparticles (Nakamura et al., 2008b), it was found that hollow CuO and NiO shrank and collapsed into solid oxides in air at 673 and 923 K, respectively, where the diffusion coefficient of slower component reaches about $10^{-22}$ m$^2$s$^{-1}$ . The temperatures at which CuO nanotubes and NiO bamboo-like structures shrank are almost consistent with these temperatures, supporting the idea that shrinking process is controlled by slower diffusion species in the case of two-component system (Gusak et al., 2005). It is not easy to estimate the diffusion coefficient of slower components of iron oxides in the shrinking process at the temperatures where shrinkage occurs because the phase transformation from $Fe_3O_4$ to γ-$Fe_2O_3$ is accompanied by shrinkage. Assuming that the shrinkage mechanism of $Fe_3O_4$ nanotubes can be simply described by a slower diffusion coefficient in $Fe_3O_4$, the diffusion coefficient of slower diffusion components, oxygen ions, can be calculated from diffusion data by Castle and Surman (1967) to be around $10^{-23}$ m$^2$s$^{-1}$ at 673-773 K where the shrinkage starts. The estimated value seems to be not so different from the $10^{-22}$ m$^2$s$^{-1}$ obtained for the slower diffusion coefficients in CuO and NiO.

### 2.2.2 Transition from iron oxide nanotube to nanoporous wires
Although $Fe_3O_4$ nanotubes shrink and collapse by annealing at higher temperatures in air as is the case with Cu- and Ni-oxides, peculiar changes in morphology occur in the process from hollow structures to collapsed structures. In this section, the unique

behaviour is reviewed. Figure 8 shows a typical example of the morphology transition of $Fe_3O_4$ nanotubes during annealing in air for 3.6 ks at (a) 673, (b) 773, and (c) 873 K. $Fe_3O_4$ nanotubes also show a tendency to shrink with increasing annealing temperature, with the nanotube structure collapsing at 873 K. It should be noted, however, that spherical nanovoids of several nanometers in diameter are also generated along the inner wall of the nanotubes at 673 K (Fig. 8(a)) and they become larger at 773 K (Fig. 8(b)). In our previous paper, we found out the experimental result supporting that the formation of the additional spherical nanovoids is closely correlated with the shrinkage of the cylindrical nanopore; the additional nanovoids appeared at 673 K, where the diameter of nanotubes started to decrease (Nakamura et al., 2009a). Furthermore, from the line profile of Fig. 8 (d) converted from the SAED patterns (a')-(c'), it is clear that $Fe_3O_4$ transforms into γ-$Fe_2O_3$ above 673 K.
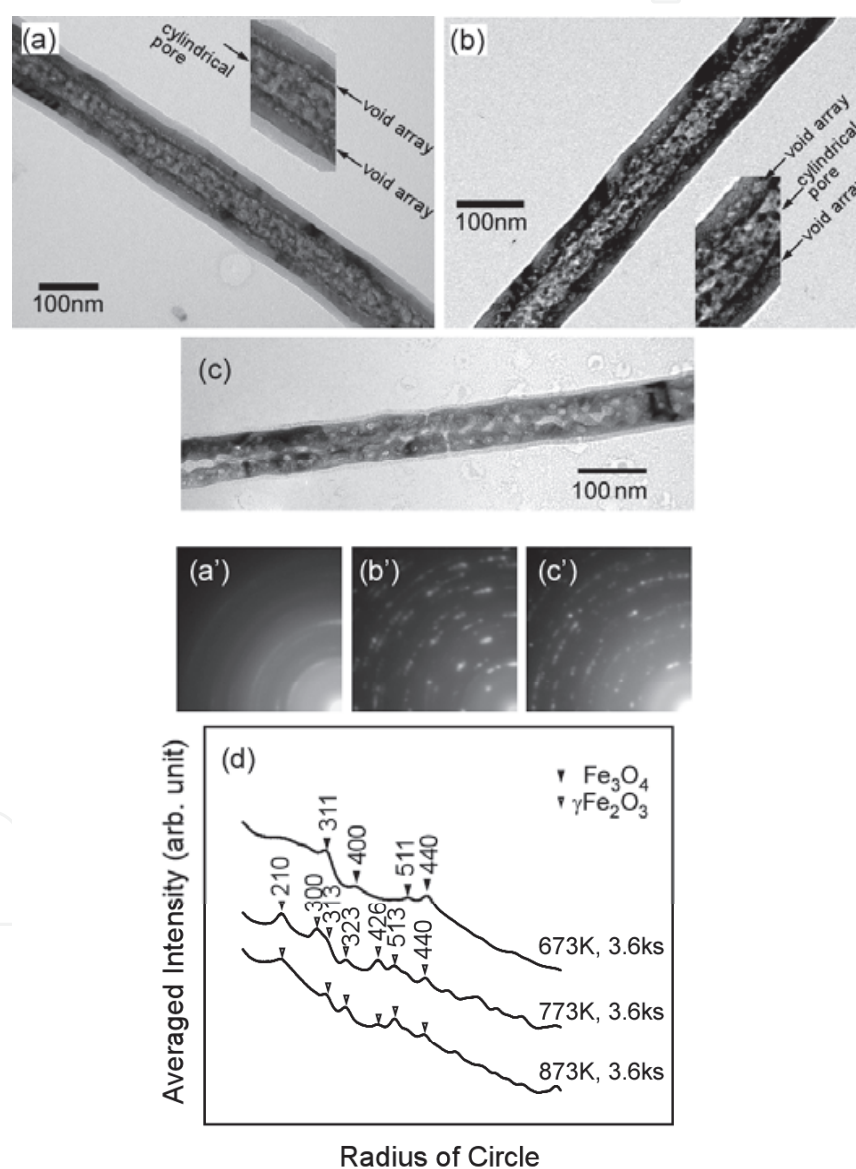


Fig. 8. A typical example of change in morphology of $Fe_3O_4$ nanotubes through annealing in air: (a) 673 K, (b) 773 K and (c) 873 K for 3.6 ks. (a')-(c') The corresponding SAED patterns and (d) the line profile of (a')-(c'). (Reproduced with permission from the references (Nakamura et al, 2009a,b))

There is a definite difference in morphology change during shirking between CuO and NiO, and $Fe_3O_4$; additional nanovoids are introduced along the inner wall of the nanotubes only in the shrinking process of $Fe_3O_4$ nanotubes. It was reported in our previous papers (Nakamura et al., 2008b) that a similar tendency can be seen in the shrinking process of hollow oxide nanoparticles; hollow CuO and NiO nanoparticles become solid particles without the formation of additional voids, whereas hollow $Fe_3O_4$ nanoparticles turn into solid $\gamma$-$Fe_2O_3$ via a porous structure (Nakamura et al., 2009a).

It should be pointed out, as mentioned above, that the phase transformation from $Fe_3O_4$ to $\gamma$-$Fe_2O_3$ proceeds when the formation of additional voids and the shrinkage of a cylindrical nanopore occur simultaneously while the crystal structure of CuO and NiO nanotubes remains unchanged in the process of shrinking. The significant difference in the shrinking process between $Fe_3O_4$ nanotubes and CuO and NiO nanotubes is attributed to the phase transformation of iron oxides.

According to Gusak et al. (2005), the shrinkage of hollow nanoparticles can be described as the outward diffusion of vacancies from the inner pores (vacancy source) to the surface (vacancy sink) of hollow nanoparticles. It is possible, therefore, to speculate that the vacancies, which generate from an inner pore, diffuse outward and then contribute to the formation of additional nano-voids. The formation of many voids of several nanometers in length along the inner wall of the $Fe_3O_4$ nanotube is regarded as evidence of the outward diffusion of vacancies from the inner cylindrical pore.

The morphology change from a $Fe_3O_4$ nanotube to porous structures is illustrated in Fig. 9; (i) vacancies diffuse outward from an interior pore as the pore shrinks, (ii) additionally spherical voids are introduced due to vacancy clustering, (iii) the shrinkage of the inner pore proceeds and the additional spherical voids grow larger, and (iv) $\gamma$-$Fe_2O_3$ nanoparticles and nanowires without nanopores were formed. This is the process by which the phase transformation from $Fe_3O_4$ to $\gamma$-$Fe_2O_3$ gradually takes place.
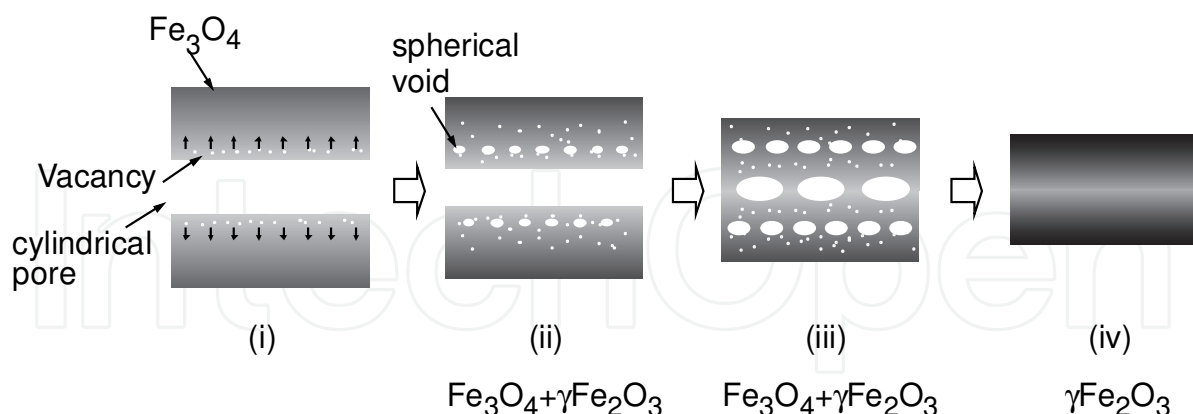


Fig. 9. Schematic illustrations of transition in the morphology of a $Fe_3O_4$ nantube: (i) dissociation and outward diffusion of vacancies at the inner surface of a nanotube of $Fe_3O_4$, (ii) formation of additional spherical voids associated with shrinkage of an interior pore and phase transformation from $Fe_3O_4$ to $\gamma$-$Fe_2O_3$, (iii) growth of voids and shrinkage of an interior pore, and (iv) the formation of nonporous $\gamma$-$Fe_2O_3$. Vacancies are generated from inner surface and diffuse outward. The outward vacancy diffusion accompanies the phase transformation from $Fe_3O_4$ to $\gamma$-$Fe_2O_3$. The vacancies combine to form voids during the diffusion process. (Reproduced with permission from the reference (Nakamura et al, 2009a))

As mentioned earlier, the phase transformation from $Fe_3O_4$ to $\gamma\text{-}Fe_2O_3$ coincides with the shrinkage of the cylindrical pore, in other words, the outward diffusion of vacancies. Sato et al. (1991) suggested that stress is induced around the boundary between $Fe_3O_4$ and $\gamma\text{-}Fe_2O_3$ in the oxidation process of $Fe_3O_4$ thin film into $\gamma\text{-}Fe_2O_3$. In the shrinking process of hollow $Fe_3O_4$, the formation of the $\gamma\text{-}Fe_2O_3$ phase seems to proceed simultaneously from the surface side to the inner side, inducing a strain field around the interface between $Fe_3O_4$ and $\gamma\text{-}Fe_2O_3$. If the strain field at the phase boundary is compressive, the vacancies that dissociate from the inner pore of the hollow particles assemble and then form a cluster around the boundary due to the tensile field of the vacancy, resulting in the relaxation of the strain around the phase boundary. Thus, the formation of additional nanovoids during the annealing of $Fe_3O_4$ nanotubes in air at high temperatures is closely related to the phase transformation from $Fe_3O_4$ and $\gamma\text{-}Fe_2O_3$. The possible formation mechanism of duplex porous iron-oxides can be described both by the outward vacancy diffusion from the nanopore and the recombination of the vacancies in the vicinity of the interface between $Fe_3O_4$ and $\gamma\text{-}Fe_2O_3$.

### 2.3 Other examples of nanotube formation via the Kirknedall effect

Another example of formation of nanotubes through the Kirkendall effect is the formation of $Ag_2Se$ nanotubes from the reaction Ag and Se ions (Bernard et al., 2006). TEM images of obtained $Ag_2Se$ nanotubes are shown in Fig. 10, together with the schematic illustrations of
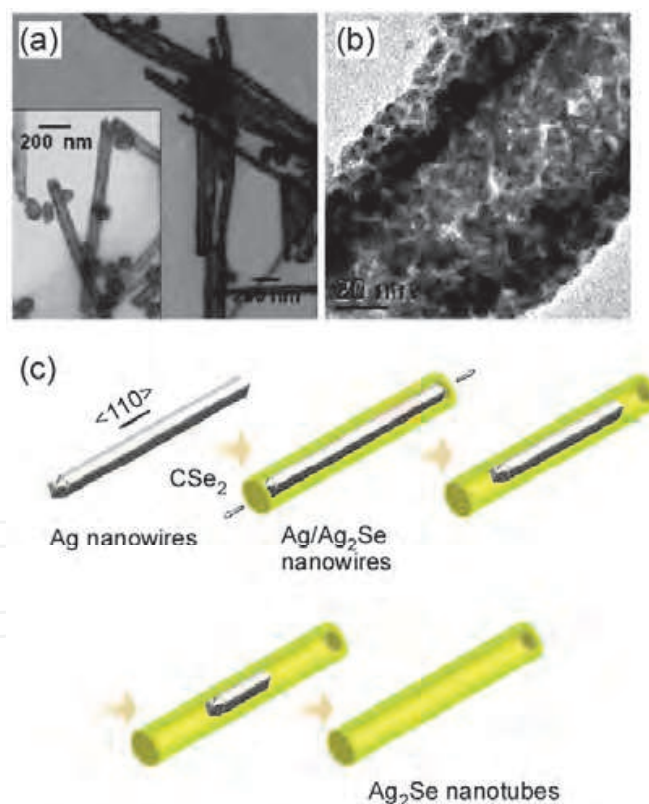


Fig. 10. $Ag_2Se$ nanotubes formed based on the Kirkendall effect. (a) TEM image of the tubes. (b) Higher-magnification view of the tube showing that the tube wall is composed of multiple grains. (c) Schematic images of the diffusion process. Due to the higher concentration of $CSe_2$ adsorbed at the end (111) faces than on the side (100) faces of the Ag nanowires, the void grows along the longitudinal <110> direction from the ends. (Reproduced with permission from the reference (Bernard et al., 2006)).

the formation process. $CSe_2$ was first adsorbed onto the surfaces of the Ag nanowire templates, and subsequent photolysis causes the dissociation of C=Se bonds, giving rise to a high surface concentration of Se atoms. $Ag_2Se$ layers are formed on the surface of Ag nanowires at 433 K and then growth of $Ag_2Se$ layers is dominated by the outward diffusion of $Ag^+$ ions through the layer. The authors mentioned that the voids were observed to grow horizontally along the wire axis rather than isotropically because the adhesion of $CSe_2$ is preferred on the ends of the Ag nanowire rather than on its side faces. Hence, the high concentration of Se atoms at the nanowire ends promotes the diffusion of $Ag^+$ along the longitudinal axis, leading to the observed anisotropic growth of vacancies along <110>. This represents a different strategy of applying the Kirkendall effect to nanotube formation from the one presented in Fig. 10.

Raidongia & Rao (2008) reported the synthesis of nanotubes of $SiO_2$, $Co_3O_4$, ZnS, CdS and CdSe by the reaction of the corresponding elemental nanowires with oxygen, sulfer and selenium due to the mechanisms of the Kirkendall effect.

## 3. Conclusion

In the past few years, there have been considerable advancements concerning the synthesis of nanowires and nanotubes. The synthesis routes based on chemical reactions such as chemical etching and galvanic replacement are broadly used for a wide variety of materials. More information on the chemical synthesis routes can be obtained in the references (Lou et al., 2008; An & Hyeon, 2009). In addition, different ideas have been applied to the fabrication of hollow nanomaterials. For example, the Kirkendall-effect related processes have been recognized as one of the useful methods for the fabrication of nanotubes of oxides, sulfides and phosphides. Since the Kirkendall effect is related to the mass transport at the interface between different solids, there is much possibility to control hollow nanostructures of a variety of alloys, intermetallic compounds and mixed oxides. The result by Fan et al. (2006), who successfully fabricated $ZnAl_2O_4$ spinel nanotubes from $ZnO/Al_2O_3$ core/shell nanowires, strongly suggests the formation of A-B alloys, compounds and mixed oxides if A/B core/shell type nanostructures are easily obtained. We can find the attempts to apply the interdiffusion processes between different oxides, which are accompanied by formation of the Kirkendall void, to the introduction of nanopipes or nanochannel inside nanowires (Marcu et al., 2010). Such basic studies are expected to increase the interests in the application nanopipes or nanochannel for DNA molecules' manipulation and investigation.

Our recent studies on the shrinkage behaviour of nanotubes are also introduced. Nanotubes of metal oxides tend to shrink and collapse at higher temperatures in oxidation atmosphere because hollow nanostructures with an inner surface are energetically unstable. Shrinking of hollow oxides occurs at temperatures where the diffusion coefficients of slower diffusing ions in the oxides are of the order of $10^{-22}$ $m^2s^{-1}$. These results suggest that it is possible to control the size of interior nanopores and particles using annealing in high temperatures. In the case of hollow iron oxide, however, a peculiar morphology change is induced in the process of shrinkage; hollow oxides with an interior spherical and cylindrical nanopore transform into porous structures with additional multiple nanovoids. Transition in porous structure seems to be related to the outward diffusion of vacancies from interior pore and

the phase transition from magnetite to maghemite. It was found by our experiments that the outward diffusion of vacancies that takes place during shrinkage contributes to the formation of a unique nanoporous structure. It should be pointed out that annealing of hollow nanostructures at high temperatures may induce further change in morphology in some cases. Further research works should be carried out to investigate the morphology change of different nanostructures at high temperature.

## 4. Acknowledgement

## 5. References

An, K. & Hyeon, T. (2009). Synthesis and biomedical applications of hollow nanostructures. *Nano Today*, Vol. 4, No. 4, pp. 359-373, ISSN 1748-0132.

Bernard Ng, C. H. Tan, H. & Fan, W. Y. (2006). Formation of $Ag_2Se$ aanotubes and Dendrite-like structures from UV irradiation of a $CSe_2$/Ag colloidal solution. *Langmuir*, Vol. 22, No. 23, pp. 9712-9717, ISSN 0743-7463

Castle, J. E. & Surman, P. L. (1967). The Self-Diffusion of Oxygen in Magnetite. *The Journal of Physical Chemistry*, Vol. 71, No. 13, pp. 4255-4259, ISSN 0022-3654

Evteev, A. V. Levchenko, E. V. Belova, I. V. & Murch, G. E. (2007). Shrinking kinetics by vacancy diffusion of a pure element hollow nanosphere. *Philosophical Magazine*, Vol. 87, No. 25, pp. 3787-3796, ISSN 1478-6435

Fan, H. J. Gösele, U. & Zacharias, M. (2007). Formation of Nanotubes and Hollow aanoparticles based on Kirkendall and diffusion processes: A review. *Small*, Vol. 3, No. 10, pp. 1660-1671, ISSN 1613-6829

Fan, H. J. Knez, M. Scholz, R. Nielsch, K. Pippel, E. Hesse, D. Zacharias, M. & Gösele, U. (2006). Monocrystalline spinel nanotube fabrication based on the Kirkendall effect. *Nature Materials*, Vol. 5, No. 8, pp. 627-631, ISSN 1476-1122

Fischer, F. D. & Svoboda, J. (2008). High temperature instability of hollow nanoparticles. *Journal of Nanoparticle Research*, Vol. 10, No. 2, pp. 255-261

Goldberger, J. He, R. Zhang, Y. Lee, S. Yan, H. Choi, H.-J. & Yang, P. (2003). Single-crystal gallium nitride nanotubes. *Nature*, Vol. 422, No. 6932, pp. 599-602, ISSN 0028-0836

Gusak, A. M. Zaporozhets, T. V. Tu, K. N. & Gösele, U. (2005). Kinetic analysis of the instability of hollow nanoparticles. *Philosophical Magazine*, Vol. 85, No. 36, pp. 4445-4464, ISSN 1478-6435

Lou, X. W. Archer, L. A. & Yang, Z. (2008). Hollow micro-/nanostructures: synthesis and applications. *Advanced Materials*, Vol. 20, No. 21, pp. 3987-4019, ISSN 1521-4095

Marcu, A. Yanagida, T. & Kawai, T. (2010). Nanochannels' fabrication using Kirkendall effect. *Solid State Sciences*, Vol. 12, No. 6, pp. 978-981, ISSN 1293-2558

Nakamura, R. Lee, J. G. Mori, H. & Nakajima, H. (2008a). Oxidation behaviour of Ni nanoparticles and formation process of hollow NiO. *Philosophical Magazine*, Vol. 88, No. 2, pp. 257 - 264, ISSN 1478-6435

Nakamura, R. Tokozakura, D. Lee, J. G. Mori, H. & Nakajima, H. (2008b). Shrinking of hollow $Cu_2O$ and NiO nanoparticles at high temperatures. *Acta Materialia*, Vol. 56, No. 18, pp. 5276-5284, ISSN 1359-6454

Nakamura, R. Matsubayashi, G. Tsuchiya, H. Fujimoto, S. & Nakajima, H. (2009a). Transition in the nanoporous structure of iron oxides during the oxidation of iron nanoparticles and nanowires. *Acta Materialia*, Vol. 57, No. 14, pp. 4261-4266, ISSN 1359-6454

Nakamura, R. Matsubayashi, G. Tsuchiya, H. Fujimoto, S. & Nakajima, H. (2009b). Formation of oxide nanotubes via oxidation of Fe, Cu and Ni nanowires and their structural stability: Difference in formation and shrinkage behavior of interior pores. *Acta Materialia*, Vol. 57, No. 17, pp. 5046-5052, ISSN 1359-6454

Raidongia, K. & Rao, C. N. R. (2008). Study of the transformations of elemental nanowires to nanotubes of metal oxides and chalcogenides through the Kirkendall effect. *The Journal of Physical Chemistry C*, Vol. 112, No. 35, pp. 13366-13371, ISSN 1932-7447

Ras, R. H. A. Kemell, M. de Wit, J. Ritala, M. ten Brinke, G. Leskelä, M. & Ikkala, O. (2007). Hollow inorganic nanospheres and nanotubes with tunable wall thicknesses by atomic layer deposition on self-assembled polymeric templates. *Advanced Materials*, Vol. 19, No. 1, pp. 102-106, ISSN 1521-4095

Ren, Y. Chim, W. K. Chiam, S. Y. Huang, J. Q. Pi, C. & Pan, J. S. (2010). Formation of nickel oxide nanotubes with uniform wall thickness by low-temperature thermal oxidation through understanding the limiting effect of vacancy diffusion and the Kirkendall phenomenon. *Advanced Functional Materials*, Vol. 20, No. 19, pp. 3336-3342, ISSN 1616-3028

Sato, M. Namikawa, T. & Yamazaki, Y. (1991). Cross-sectional observation of $Fe_3O_4$-gamma-$Fe_2O_3$ intermediate thin-films. *Japanese Journal of Applied Physics*, Vol. 30, No. 3B, pp.L489-491, ISSN 0021-4922

Shen, G. Bando, Y. Ye, C. Yuan, X. Sekiguchi, T. & Golberg, D. (2006). Single-Crystal Nanotubes of II3-V2 Semiconductors. *Angewandte Chemie International Edition*, Vol. 45, No. 45, pp. 7568-7572, ISSN 1521-3773

Smigelskas, A. D. & Kirkendall, E. O. (1947). Zinc diffusion in alpha brass. Trans. AIME, Vol. 171, No., pp. 130-142

Tu, K. N. & Gösele, U. (2005). Hollow nanostructures based on the Kirkendall effect: Design and stability considerations. *Applied Physics Letters*, Vol. 86, No. 9, pp., ISSN 0003-6951

Yin, Y. Rioux, R. M. Erdonmez, C. K. Hughes, S. Somorjai, G. A. & Alivisatos, A. P. (2004). Formation of hollow nanocrystals through the nanoscale Kirkendall effect. *Science*, Vol. 304, No. 5671, pp. 711-714

**Nanowires - Implementations and Applications**

Edited by Dr. Abbass Hashim

This potentially unique work offers various approaches on the implementation of nanowires. As it is widely known, nanotechnology presents the control of matter at the nanoscale and nanodimensions within few nanometers, whereas this exclusive phenomenon enables us to determine novel applications. This book presents an overview of recent and current nanowire application and implementation research worldwide. We examine methods of nanowire synthesis, types of materials used, and applications associated with nanowire research. Wide surveys of global activities in nanowire research are presented, as well.

**How to reference**

In order to correctly reference this scholarly work, feel free to copy and paste the following:

# INTECH
open science | open minds